

Freezing, melting and the onset of glassiness in binary mixtures

Daniele Coslovich,^{1,*} Leonardo Galliano,¹ and Lorenzo Costigliola²

¹*Dipartimento di Fisica, Università di Trieste, Strada Costiera 11, 34151, Trieste, Italy*

²*“Glass and Time”, IMFUFA, Department of Science and Environment,
Roskilde University, P.O. Box 260, DK-4000 Roskilde, Denmark*

(Dated: June 10, 2024)

We clarify the relationship between freezing, melting and the onset of glassy dynamics in the prototypical glass-forming Kob-Andersen mixture. Our starting point is a precise definition of the onset of glassiness, as expressed by the emergence of an inflection in the time-dependent correlation functions. By scanning the temperature-composition phase diagram of the model, we find that the onset temperature barely varies with concentration, unlike the freezing temperature, which shows a marked drop at the eutectic point. We observe, however, a surprising correspondence between the onset of glassiness and the solidus line, along which the underlying crystalline phases melt. At fixed concentration, the freezing and onset temperatures display similar pressure dependencies, which are very well predicted by the isomorph theory and are encoded in the variation of the excess entropy. While our results rule out a general connection between thermodynamic metastability and glassiness, they call for a careful assessment of the role of crystalline precursors in glass-forming liquids.

Two-step relaxation is one of the most prominent features of disordered materials in the proximity of a glass transition [1]. It is readily inferred from the presence of a plateau in time-dependent correlation functions and reflects the strong separation of time scales between fast microscopic motion and a spectrum of much slower relaxation processes. In a thermal cooling process, the appearance of two-step relaxation defines a crossover temperature T_0 , which marks the onset of slow dynamics [2] or, as we shall write in the following, “onset of glassiness” [1]. Below T_0 , in fact, the system ceases to be a normal liquid and develops the typical features of glassy dynamics, including dynamic heterogeneity and super-Arrhenius dependence of relaxation times, which eventually lead to dynamical arrest at the glass transition temperature $T_g < T_0$. Predicting and explaining the origin of these features in materials as diverse as supercooled liquids [3], spin glasses [4] or type-II superconductors [5] is a key challenge in the field of disordered systems.

One important and yet often eluded question is whether the onset of glassiness is related or not to thermodynamic metastability with respect to an ordered crystalline phase. From a theoretical standpoint, a connection between the onset of glassiness and crystallization has been invoked in a phenomenological model of the glass transition [6]. In a similar vein, the so-called frustration-limited domains theory [7] attributes the onset of glassiness to an avoided crystallization, which occurs however in a curved space where geometric frustration is lifted. On the other hand, in theoretical approaches based on mean-field spin glass models or infinite-dimensional systems [8] crystallization is ruled out from the outset, and the onset of glassiness is related to the appearance of amorphous metastable states and activated transitions between them [9, 10]. Most other theories of the glass transition [3] also neglect the role of crystallization.

From an empirical point of view, it is clear that thermodynamic metastability is not a necessary condition for glassy dynamics: silica, for instance, is a highly viscous liquid already at its melting temperature T_m [11], and a similar discrepancy

is observed in B_2O_3 and glycerol [12–14]. A connection between crystallization and the onset of glassiness may nonetheless hold within subsets of liquids with similar intermolecular interactions [15]. Previous analysis of experimental data [16] indicated a rough correlation between the melting temperature T_m and a crossover temperature T_A , akin to T_0 , at which super-Arrhenius behavior sets in [17]. Recent simulation studies of a prototypical Lennard-Jones (LJ) binary mixture even suggested an identity, $T_m \approx T_0$ [18, 19]. In multi-component systems, however, the liquid phase can be metastable with respect to a pure crystal, to coexisting liquid and crystal phases or to phase-separated crystals, and freezing and melting transitions must be clearly distinguished. These aspects have not been addressed in any detail so far. There are also indications that thermodynamic properties related to the excess entropy [20] change sharply around the onset temperature [18]. Our goal is to clarify these connections in a glassy binary mixture with different chemical compositions, disentangling the role of melting and freezing, and to provide the basis for a systematic analysis on a broader range of liquids.

One technical hurdle to tackle is the determination of the onset temperature T_0 , for which there is no generally-agreed, operational definition. The appearance of super-Arrhenius dependence of relaxation times can be used as a proxy for the onset temperature, but such a procedure is often done “by eye” or making assumptions about the functional form of $\tau(T)$ [7, 17, 21]. The onset of glassiness is also associated to a decrease of the inherent structure energy upon decreasing temperature [2, 9], but the crossover is broad and does not provide a clear-cut definition. Alternative but more complex procedures have also been proposed [22]. In the following, we will provide a straightforward and precise definition of the onset of glassiness in terms of the critical points of time-dependent correlation functions. Our procedure removes the above difficulties and is generally applicable to both simulation and experimental data, as it does not require knowledge of the interaction model.

In this work, we study in detail the composition dependence

of the onset of glassiness in the paradigmatic case of the Kob-Andersen (KA) mixture [23], which is a simple LJ mixture of two types of particles, A and B . The concentration of B particles is x , with $x = 0.2$ corresponding to the canonical KA mixture. We performed molecular dynamics simulations for a KA mixture composed of $N = 500$ particles along constant pressure paths, using the `atooms` simulation framework [24]. We used a reproducible computational workflow, available in the associated dataset [25]. We controlled the pressure P during the equilibration run using a Berendsen barostat, paying attention to removing drift of the center of mass. We performed the production runs with a Nose-Poincaré thermostat [26], fixing the volume to the average volume measured during the second half of the equilibration run. We also performed some runs along constant density paths, fixing the density at the one determined at the freezing temperature T_f [19]. As a cross-check, we did additional simulations for a larger system size ($N = 8000$) using RUMD [27] employing a different numerical integrator for the constant-pressure simulations [28]. More details are given in the Supplemental Material (SM) [29].

We compute the self intermediate scattering functions $F_s(k, t)$ for the A -particles (the results for the B -particles are qualitatively similar and are included in the SM). We focus on wave-vectors k in the range of the first peak of the structure factor $S_{AA}(k)$. The calculation of the time derivative $F'_s(k, t)$ requires some care as it can be affected by statistical noise: to cope with this, we first compute $tF'_s(k, t)$ numerically, then fit it to a 4th order polynomial, restricting the time range such that F_s is between 0.05 and 0.98, and extract the critical points from it. The onset is signaled by the presence of a two-minima structure of $tF'_s(k, t)$. The height δ of the smallest barrier separating the two minima of tF'_s defines a precise, observable-dependent order parameter for the onset of glassiness: it becomes finite below T_0 . The non-ergodicity factor can then be defined as $F_s(k, t^*)$, where t^* is the time corresponding to the maximum of tF'_s , and jumps discontinuously at T_0 . The necessary software is available with the accompanying dataset [25].

Our procedure is illustrated in Fig. 1 for the canonical concentration $x = 0.2$ at a pressure $P = 10.19$. We start by equilibrating the system at high temperature, well within the liquid phase, and then decrease the temperature at fixed pressure until $\delta > 0$. Once T_0 has been bracketed, we perform additional simulations to refine its determination. Panel (a) displays the intermediate scattering functions for $k = 7.2$ around the onset temperature. The very definition of the onset can be grasped from panel (b) and (c): the time derivatives $tF'_s(k, t)$ display a monotonic behavior above T_0 and (at least) one local maximum below T_0 , corresponding to an inflection of $F_s(k, t)$. The polynomial fit, indicated by solid lines, is fairly robust and works well even with noisy data [29]. Small oscillations in $tF'_s(k, t)$ at short times, unrelated to the onset of glassiness [29, 30], are visible with high-quality statistics, but they do not affect the calculation of δ . To locate T_0 precisely, we fit $\delta(T)$ to a linear function that vanishes at T_0 . A simpler bisection procedure, which does not involve any fit, is also possible and provides consistent results [29]. Finally, we show

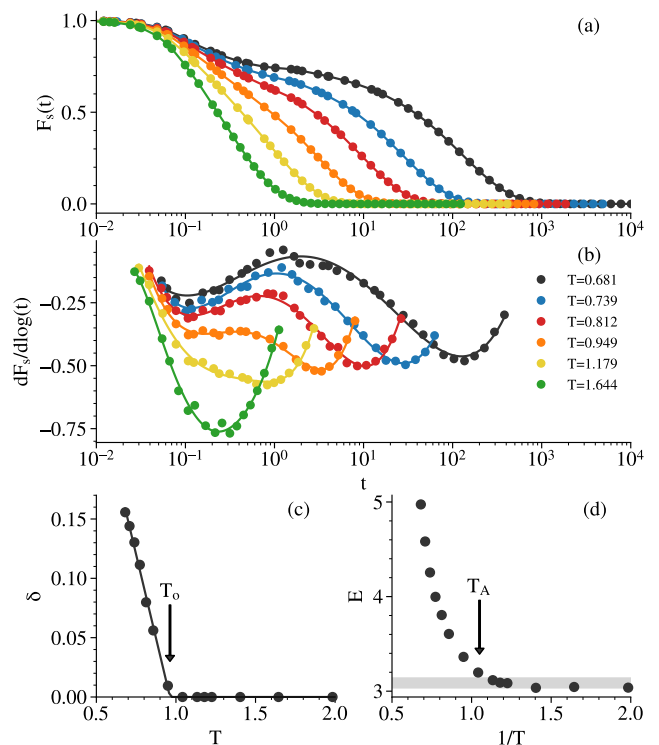


FIG. 1. Overview of the protocol to define the onset temperature, illustrated along the isobar $P = 10.19$ at the concentration $x = 0.2$: (a) $F_s(k, t)$ of A -particles for selected temperatures around T_0 at $k = 7.2$; (b) derivative $tF'_s(k, t)$ for the same temperatures as in (a), the solid lines are 4th order polynomial fits; (c) order parameter δ obtained from $tF'_s(k, t)$ as a function of T , the solid line is a linear fit vanishing at T_0 ; (d) activation energy $E(T) = T \log(\tau_\alpha/\tau_\infty)$ as a function of T . In panel (c) and (d), the vertical arrows mark the onset temperature and the crossover temperature from Arrhenius to super-Arrhenius behavior, respectively. In panel (d), the shaded area indicates the approximate range of validity of the high-temperature Arrhenius fit.

in panel (e) the activation energy $E(T) = T \log(\tau_\alpha/\tau_\infty)$ [7] associated to the structural relaxation times $\tau_\alpha(T)$, at which $F_s(k, \tau_\alpha) = 1/e$. The microscopic time τ_∞ is obtained by fitting the high-temperature portion of the data to an Arrhenius equation. As expected, the onset of two-step relaxation is accompanied by the appearance of super-Arrhenius temperature dependence at some temperature T_A . We find that T_A is slightly larger than T_0 , by about 10% to 20% depending on composition, and is also sensitive to the range of the Arrhenius fit, which holds anyway only approximately at high temperature [31].

We now turn to the relationship between the onset of glassiness and crystallization. The phase diagram of the KA mixture has been studied by Pedersen *et al.* [19] for compositions in the range $0 < x < 0.5$. It displays the typical features of eutectic mixtures: the freezing (or “liquidus”) line, along which the liquid phase coexists with pure crystals of either fcc or CsCl symmetry, has a minimum at an eutectic point located around $x = 0.25$. Around this composition, however,

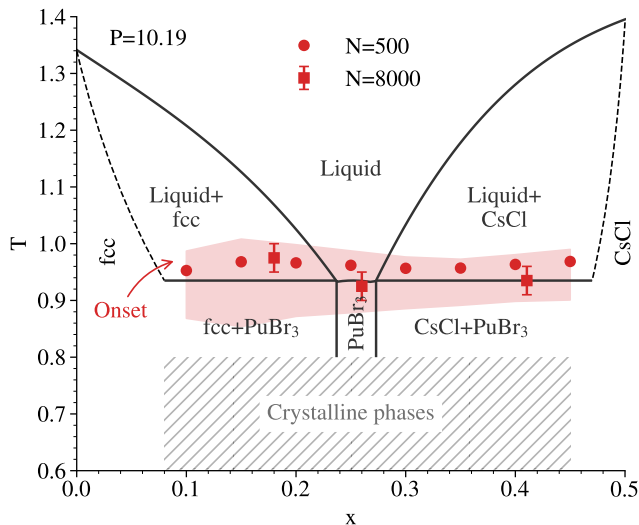


FIG. 2. Onset temperatures T_0 for $N = 500$ (circles) and $N = 8000$ (squares) as a function of concentration of B-particles x . The shaded area indicates the range of T_0 obtained for different values of k in the range $[5, 10]$, around the first peak of $S_{AA}(k)$. The full lines are the phase diagram inferred from Ref. 19, along with the corresponding stable phases. The dashed lines are sketches of the stability limits of the pure crystalline phases.

the stable crystalline phase has a PuBr_3 symmetry [19]. We reproduce these results as solid lines in Fig. 2. We also trace the melting (or “solidus”) lines, along which the crystalline phases melt, as inferred from Ref. 19. The low-temperature portion of the phase diagram is instead unknown. We superpose on the phase diagram the onset temperatures obtained from the protocol described above. The shaded area indicates the range of onsets corresponding to k values around the first peak of $S_{AA}(k)$, i.e., from $k = 5$ to 10, while the filled points are for $k = 7.2$. It is clear that the locus of T_0 does not track the freezing line: while the latter displays the typical V-shape of eutectic mixtures, T_0 does not show any systematic variation with x . Qualitatively similar results are observed for the B-particles, for which T_0 only shows a slight increase as a function of x .

The qualitatively different trends of T_f and T_0 demonstrate that the onset of glassiness and freezing are not directly connected in the KA mixture: the system can be thermodynamically metastable *without being glassy*. Results for a different pressure $P = 30$ lead to the same conclusions [29]. Surprisingly, however, the onset of glassiness closely follows the solidus line, which runs horizontally in the diagram: above this line, the stable crystalline structures melt at least partially. At this stage, we emphasize that the correspondence of the onset temperature with the melting of the underlying stable crystal phases could be coincidental. Proving a causal connection would require a direct determination of crystalline precursors in the metastable liquid – we will come back to this point in the closing paragraphs.

The results shown in Fig. 2 also allow us to dissipate a

possible source of confusion. Pedersen *et al.* [19] reported that for $x = 0.2$ the melting temperature coincided with T_0 , as determined from the appearance of super-Arrhenius behavior [21]. In Ref. [19], however, no clear distinction was made between melting and freezing. As we can see from Fig. 2, $T_m \approx T_f \approx T_0$ around the eutectic composition, but deviations are found for other values of x . An approximate identity between T_0 and T_m holds in the KA mixture, but for a different reason from the one implied by Ref. 19. We also note that the absence of a direct connection between T_f and T_0 may be partly inferred from the trends of the iso-diffusivity lines shown in Ref. 19, which only show a weak, monotonic dependence on x . We obtained indeed similar results for the relaxation time itself [29]. However, transport coefficients *per se* do not provide direct information about the shape of time-dependent correlation functions.

Even though the freezing line does not track the onset of glassiness in the x - T diagram, T_f and T_0 scale similarly at fixed concentration as a function of pressure. This is shown in Fig. 3 for selected concentrations. We have used a constant wave-vector $k = 7.2$ for the calculation of the onset, independent of composition. Interestingly, it is possible to accurately predict the pressure dependence of both quantities using the isomorph theory [32]. Following Ref. [19], we predict $T_f(P)$ at any fixed x_B from the knowledge of $T_f(P_0 = 10.19)$ using the equation $T/T_0 = (\gamma_0/2 - 1)(\rho/\rho_0)^4 - (\gamma_0/2 - 2)(\rho/\rho_0)^2$ [33] together with $P/\rho = k_B T + (2w_0 - 4u_0)(\rho/\rho_0)^4 - (w_0 - 4u_0)(\rho/\rho_0)^2$ [34], where ρ and ρ_0 are the densities corresponding to P and P_0 , respectively, and w_0 and u_0 are the values of the per-particle virial and potential energy at the state point (ρ_0, T_0) . The agreement is excellent for T_0 , indicating that its pressure dependence can be explained in terms of the hidden scale invariance of the LJ potential [32]. The agreement for T_f is still very good, but slightly worse for $x = 0.638$, in agreement with Ref. 19. This is consistent with the observation that freezing line is an isomorph only to good approximation, but not exactly [35].

Is it possible to predict the onset temperature from other thermodynamic properties of the system? Previous works have connected the onset of glassiness to a change in the n -body contributions to the excess entropy s_{ex} per particle, which is defined as the difference between the total entropy and its ideal gas contribution [20, 36]. More precisely, the residual many-body entropy (RMBE) is defined as $\Delta s = s_{\text{ex}} - s_2$, where s_2 is the two-body approximation to s_{ex} [37]. It has been found that in the KA mixture Δs changes sign upon cooling at a temperature slightly lower than T_0 [36]. Note that $\Delta s = 0$ has also been proposed as an empirical criterion for freezing in one-component liquids [38], see also Ref. 39.

We now critically revisit the connection between the onset of glassiness and excess entropy for the KA mixture by calculating s_{ex} and s_2 along isobaric paths at $P = 10.19$ over a range of compositions. For each value of x , the calculation is carried out by thermodynamic integration from a low-density, high-temperature state ($\rho = 10^{-4}$, $T = 5$), where we assume that the system behaves like an ideal gas [36]. We fol-

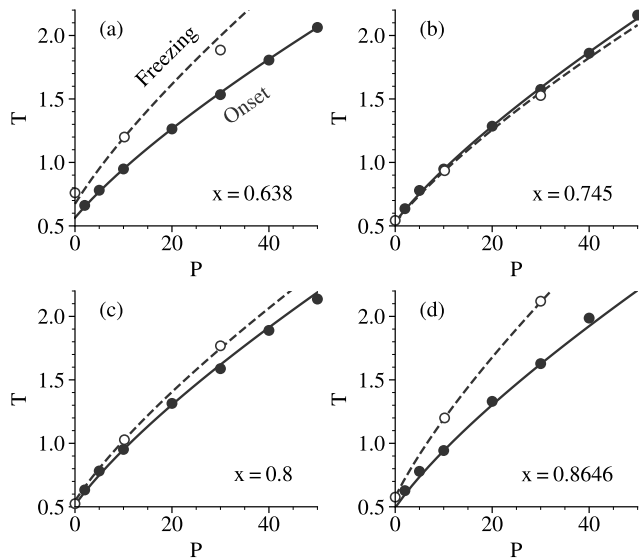


FIG. 3. Pressure dependence of the freezing temperature T_f (open circles) and of the onset temperature T_o (filled circles) for several concentrations, as indicated in the panels. The theoretical predictions for T_f and T_o obtained from the isomorph theory are shown as dashed and solid lines, respectively.

low both constant-density and constant-pressure paths. In this latter kind of path, we first follow an isothermal path at $T = 5$ up to density $\rho = \rho(T = 5, P = 10.19)$ and then proceed with batches of small isothermal and isochoric paths, keeping the system along the selected isobar. As a check, we compared the excess entropy obtained via this procedure for $x = 0.2$ and $x = 0.35$ with the one along isochoric paths terminating at a common state point, and found very good agreement (less than 1% difference). We also compared our results for s_{ex} agree within error bars with those of Bell *et al.* [20]. Our results for Δs around the canonical density $\rho = 1.2$ agree for s_2 within a few percents with the those in Ref. [36]. These discrepancies are likely due to slight differences in the integration path.

Excess entropy data are shown in Fig. 4 in the temperature-composition diagram. Interestingly, the lines at constant excess entropy display the same qualitative behavior as the onset of glassiness, namely they vary weakly with x at constant pressure and are non-monotonic, with a maximum around the eutectic point at constant density. This behavior is in line with the quasi-universality of excess entropy scaling put forth by Bell *et al.* [20]: the excess entropy provides an approximate scaling of the dynamics across *different* liquids. This is confirmed by the excess entropy scaling of the structural relaxation times [29]. In particular, the value of the excess entropy at T_o is quasi-universal and lies between -4.8 and -5.0. Combining these observations with those inferred from Fig. 2, we conclude that melting occurs in this same range of excess entropies, irrespective of x . The melting temperature would then be a quasi-universal property in the sense of Ref. 20, but the

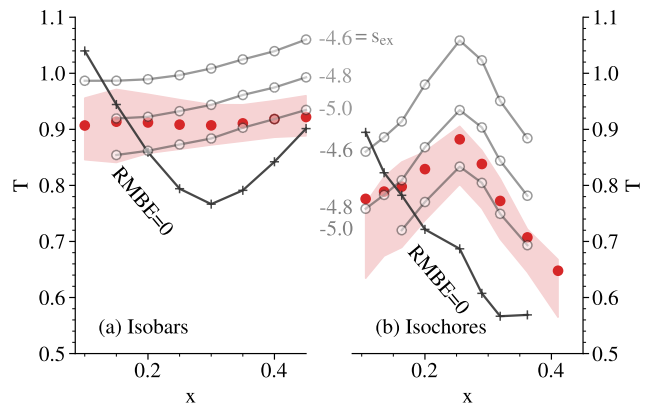


FIG. 4. Excess entropy measures in the temperature-concentration diagram for (a) isobaric paths at $P = 10.19$ and (b) isochoric paths at densities corresponding to freezing, $\rho(T = T_f, P = 10.19, x)$. In both panels, the temperatures at which $s_{\text{ex}} = \text{const}$ and $\Delta s = 0$ are indicated as open empty circles and crosses, respectively. The onset temperatures T_o are included with the same representation as in Fig. 2.

freezing one not.

To investigate the putative connection between the excess entropy, crystallization and the onset of glassiness, we also include in Fig. 4 the temperatures at which Δs vanishes [36]. The first observation is that the locus of points where $\Delta s = 0$ has a non-monotonic behavior, with a minimum around the eutectic composition. This trend is thus qualitatively similar to the one of the freezing line, cf. Fig. 2, but Δs vanishes at a temperature lower than T_f by 10–50% depending on composition. It is also clear that $\Delta s = 0$ does not provide a physically sound criterion for the onset of glassiness, which occurs instead around the same temperature irrespective of x . Similar discrepancies are observed on paths at constant density, see panel (b), where ρ is fixed for each composition at the density corresponding to the freezing temperature at $P = 10.19$ [19]. The surprising non-monotonic behavior of T_o is well reproduced by the lines at constant s_{ex} , while those for which $\Delta s = 0$ display a qualitatively different trend. Therefore, the splitting of s_{ex} into two-body and many-body contributions does not bear any clear connection with the onset of glassiness in the KA mixture.

One conclusion to be drawn from our work is the lack of a general connection between thermodynamic metastability and the onset of glassiness. Not only a liquid can be glassy and highly viscous without being metastable, as is the case for silica: the large gap between T_f and T_o seen in Fig. 2 shows that a liquid can also be metastable without being glassy. Key to this observation is the distinction between freezing and melting, which has not been duly taken into account so far in computational studies of the KA mixture. Nonetheless, in the KA mixture all characteristic temperatures scale similarly with pressure at fixed concentration, see Fig. 3, in agreement with the predictions of the isomorph theory. When using pressure as an implicit variable, we thus expect a broad correlation between

T_o and crystallization temperatures in all systems with isomorph invariance [32], such as van der Waals liquids, weakly ionic or dipolar liquids and metals.

The second key observation is that the onset of glassiness occurs close to the solidus line, which marks the melting of the underlying crystalline phases. The generality of this connection can now be tested straightforwardly for simple computational models whose phase diagram is known [40–42]. In particular, we did preliminary calculations for the Wahnström LJ mixture, whose phase diagram has been determined recently [43], and we found very similar results to those presented therein: in particular, T_o and T_m are very close to one another. Note that our method to determine T_o can also be easily adapted to experiments, where precise measurements of the onset temperature are rare, see Ref. 44 for an exception.

Our findings motivate a critical reassessment of the role of local structure in glass-forming liquids [45–47]. It has been argued that the competition between crystalline precursors, corresponding to different crystalline phases, can contribute to stabilize the metastable liquid [41]. In this respect, it would be interesting to identify precursors of the PuBr₃ phase in the KA mixture, as this phase is stable very close to the fcc-CsCl eutectic composition. This crystal structure contains bicapped prismatic structures akin to the putative locally favored structure [48] and has been so far been overlooked in crystallization studies of the KA model [49–51]. Structural analysis across the melting line will provide a crucial numerical test of the role of crystalline precursors.

Finally, on the theoretical side, it would be worth revisiting the conjecture that T_o coincides with the *exact* critical temperature of the ideal mode-coupling theory [9] and investigating whether recent extensions of the theory [52, 53] can predict the onset temperature. Another promising approach to rationalize the onset of glassiness builds on the relationship between short-time dynamics and the local curvature of the potential energy surface, see Refs. 54 and 55 for recent work in this direction. Predicting when liquids first start to show glassy behavior is a well-defined and important open problem for theories of the glass transition [1]. Our work lays down the necessary basis to address this problem quantitatively.

ACKNOWLEDGMENTS

We thank Jeppe Dyre, Walter Kob and Ulf Pedersen for useful discussions. LC thanks support from VILLUM Foundation *Matter* grant (No. 16515). The article has been produced with co-funding from the European Union - Next Generation EU. The data and workflow necessary to reproduce the findings of this study will be available after publication of the paper in the Zenodo data repository [25].

* dcoslovich@units.it

- [1] A. Cavagna, *Phys. Rep.* **476**, 51 (2009), 0903.4264.
- [2] S. Sastry, P. G. Debenedetti, and F. H. Stillinger, *Nature* **393**, 554 (1998).
- [3] L. Berthier and G. Biroli, *Rev. Mod. Phys.* **83**, 587 (2011).
- [4] A. P. Young, *Spin Glasses and Random Fields* (World Scientific, 1998).
- [5] T. Nattermann and S. Scheidl, *Adv. Phys.* **49**, 607 (2000).
- [6] H. Tanaka, *J. Chem. Phys.* **111**, 3163 (1999).
- [7] G. Tarjus, S. A. Kivelson, Z. Nussinov, and P. Viot, *J. Phys.: Condens. Matter* **17**, R1143 (2005).
- [8] G. Parisi, P. Urbani, and F. Zamponi, *Theory of Simple Glasses: Exact Solutions in Infinite Dimensions* (Cambridge University Press, New York, 2020).
- [9] Y. Brumer and D. R. Reichman, *Phys. Rev. E* **69**, 041202 (2004).
- [10] G. Biroli and J.-P. Bouchaud, in *Structural Glasses and Supercooled Liquids* (John Wiley & Sons, Ltd, 2012) Chap. 2, pp. 31–113.
- [11] G. Urbain, Y. Bottinga, and P. Richet, *Geoch. Cosm. Acta* **46**, 1061 (1982).
- [12] E. Rössler, A. P. Sokolov, A. Kisliuk, and D. Quitmann, *Phys. Rev. B* **49**, 14967 (1994).
- [13] J. Wuttke, J. Hernandez, G. Li, G. Coddens, H. Z. Cummins, F. Fujara, W. Petry, and H. Sillescu, *Phys. Rev. Lett.* **72**, 3052 (1994).
- [14] J. Wuttke, W. Petry, G. Coddens, and F. Fujara, *Phys. Rev. E* **52**, 4026 (1995).
- [15] R. J. Greet and J. H. Magill, *J. Phys. Chem.* **71**, 1746 (1967).
- [16] H. Tanaka, *J. Chem. Phys.* **111**, 3175 (1999).
- [17] C. Hansen, F. Stickel, T. Berger, R. Richert, and E. W. Fischer, *J. Chem. Phys.* **107**, 1086 (1997).
- [18] A. Banerjee, M. K. Nandi, S. Sastry, and S. Maitra Bhattacharyya, *J. Chem. Phys.* **147**, 024504 (2017).
- [19] U. R. Pedersen, T. B. Schröder, and J. C. Dyre, *Phys. Rev. Lett.* **120**, 165501 (2018).
- [20] I. H. Bell, J. C. Dyre, and T. S. Ingebrigtsen, *Nat. Commun.* **11**, 4300 (2020).
- [21] D. Coslovich and G. Pastore, *J. Chem. Phys.* **127**, 124505 (2007).
- [22] S. S. Schoenholz, E. D. Cubuk, D. M. Sussman, E. Kaxiras, and A. J. Liu, *Nat. Phys.* **12**, 469 (2016).
- [23] W. Kob and H. C. Andersen, *Phys. Rev. E* **52**, 4134 (1995).
- [24] D. Coslovich, “atooms: A framework for simulations of interacting particles (3.22.0),” (2017–2024).
- [25] D. Coslovich, L. Galliano, and L. Costigliola, “Dataset: Freezing, melting and the onset of glassiness in binary mixtures,” (2024), the dataset will be deposited upon acceptance.
- [26] S. Nose, *J. Phys. Soc. Jap.* **70**, 75 (2001).
- [27] N. Bailey, J. S. Hansen, T. Ingebrigtsen, A. Veldhorst, L. Bøhling, C. Lemarchand, A. Olsen, A. Bacher, L. Costigliola, U. Pedersen, H. Larsen, J. Dyre, and T. Schröder, *SciPost Phys.* **3**, 038 (2017).
- [28] G. J. Martyna, D. J. Tobias, and M. L. Klein, *J. Chem. Phys.* **101**, 4177 (1994).
- [29] See Supplemental Material at <https://> for simulation details, additional analysis and tabulated data.
- [30] V. V. Brazhkin, Y. D. Fomin, A. G. Lyapin, V. N. Ryzhov, E. N. Tsiok, and K. Trachenko, *Phys. Rev. Lett.* **111**, 145901 (2013).
- [31] L. Costigliola, U. R. Pedersen, D. M. Heyes, T. B. Schröder, and J. C. Dyre, *J. Chem. Phys.* **148**, 081101 (2018).
- [32] T. S. Ingebrigtsen, T. B. Schröder, and J. C. Dyre, *Phys. Rev. X* **2**, 011011 (2012).
- [33] T. S. Ingebrigtsen, L. Bøhling, T. B. Schröder, and J. C. Dyre, *J. Chem. Phys.* **136**, 061102 (2012).

- [34] T. B. Schröder, N. Gnan, U. R. Pedersen, N. P. Bailey, and J. C. Dyre, *J. Chem. Phys.* **134**, 164505 (2011).
- [35] U. R. Pedersen, L. Costigliola, N. P. Bailey, T. B. Schröder, and J. C. Dyre, *Nat. Commun.* **7**, 12386 (2016).
- [36] M. Singh, M. Agarwal, D. Dhabal, and C. Chakravarty, *J. Chem. Phys.* **137**, 024508 (2012).
- [37] A. Baranyai and D. J. Evans, *Phys. Rev. A* **40**, 3817 (1989).
- [38] P. V. Giaquinta, G. Giunta, and S. Prestipino Giarritta, *Phys. Rev. A* **45**, R6966 (1992).
- [39] W. P. Krekelberg, V. K. Shen, J. R. Errington, and T. M. Truskett, *J. Chem. Phys.* **128**, 161101 (2008).
- [40] M. Yiannourakou, I. G. Economou, and I. A. Bitsanis, *J. Chem. Phys.* **130**, 194902 (2009).
- [41] J. Russo, F. Romano, and H. Tanaka, *Phys. Rev. X* **8**, 021040 (2018).
- [42] V. Molinero, S. Sastry, and C. A. Angell, *Phys. Rev. Lett.* **97**, 075701 (2006).
- [43] K. Nishio, *Phys. Rev. E* **109**, 044110 (2024).
- [44] B. Schmidtke, N. Petzold, R. Kahlau, and E. A. Rössler, *J. Chem. Phys.* **139**, 084504 (2013).
- [45] C. P. Royall and S. R. Williams, *Phys. Rep.* **560**, 1 (2015).
- [46] H. Tanaka, H. Tong, R. Shi, and J. Russo, *Nat. Rev. Phys.* **1**, 333 (2019).
- [47] D. Wei, J. Yang, M.-Q. Jiang, L.-H. Dai, Y.-J. Wang, J. C. Dyre, I. Douglass, and P. Harrowell, *J. Chem. Phys.* **150**, 114502 (2019).
- [48] D. Coslovich, *Phys. Rev. E* **83**, 051505 (2011).
- [49] P. Crowther, F. Turci, and C. P. Royall, *J. Chem. Phys.* **143**, 044503 (2015).
- [50] U. K. Nandi, A. Banerjee, S. Chakrabarty, and S. M. Bhat-tacharyya, *J. Chem. Phys.* **145**, 034503 (2016).
- [51] T. S. Ingebrigtsen, J. C. Dyre, T. B. Schröder, and C. P. Royall, *Phys. Rev. X* **9**, 031016 (2019).
- [52] C. Luo and L. M. C. Janssen, *J. Chem. Phys.* **153**, 214507 (2020).
- [53] S. Ciarella, C. Luo, V. E. Debets, and L. M. C. Janssen, *Eur. Phys. J. E* **44**, 91 (2021).
- [54] G. Sun and P. Harrowell, *J. Chem. Phys.* **157**, 024501 (2022).
- [55] D. Coslovich and A. Ikeda, *J. Chem. Phys.* **156**, 094503 (2022).